J Supercond Nov Magn (2016) 29:981–984
DOI 10.1007/s10948-016-3392-7

ORIGINAL PAPER

Preparation and Magnetic Properties of La-Substituted Strontium Hexaferrite by Microwave-Assisted Sol-Gel Method

Zhanyong Wang[1] · Wenya Yang[1] · Zhipeng Zhou[1] · Minglin Jin[1] · Jiayue Xu[1] · Yanli Sui[2]

Received: 15 October 2015 / Accepted: 6 January 2016 / Published online: 18 January 2016

Abstract $Sr_{1-x}La_xFe_{12}O_{19}$ ($x = 0$, 0.15, 0.25, 0.5) hexaferrites were prepared by microwave-assisted sol-gel method. The thermal decomposition process, structural, and magnetic properties of the products were studied by thermal differential scanning calorimeter (DSC), thermogravimetry (TG), X-ray diffraction (XRD), and vibrating sample magnetometer (VSM). The phase of α-Fe_2O_3 appeared at $x = 0.25$ and $x = 0.5$. The coercivity of La^{3+}-substituted strontium hexaferrites is improved to 5960.2 Oe at $x = 0.25$.

Keywords Microwave-assisted calcination · M-strontium hexaferrites · Sol-gel · La doping

1 Introduction

M-strontium hexaferrites have been widely used in communication, electromagnetic wave absorbers, and magnetic recording medium for their good chemical stability, high magnetization, excellent corrosion resistivity, and low manufacturing cost [1–5]. The magnetization and intrinsic magnetic properties of $SrFe_{12}O_{19}$ hexaferrites result from the unfinished offset of Fe^{3+} magnetic moment and the partial substitution for Sr^{2+} sites in different crystallographic sites, respectively [6, 7]. The rare earth elements, such as La^{3+} [6, 7], usually were used to replace the Sr^{2+} of crystallographic sites to modify the coercivity. Many previous studies focused on the improvement of the magnetic characteristics by the preparation of thin films and submicron particles [8–10]. Sol-gel auto-combustion is an advanced preparation method of ultrafine power because of cheap precursor, low reaction temperature, and accurate control of material composition. Moreover, the process of calcination has great effects on magnetic properties. Microwave-assisted synthesis has been paid more attention since the first discussion in 1986 [11–14]. The heating energy in the process of microwave-assisted calcination derives from the interaction between materials and microwave, instead of originating from external sources, which can improve the diffusion coefficient, reduce calcination temperature, shorten reaction time, and endow materials with some new characteristics [15]. In this work, the structural, magnetic properties of La-substituted strontium hexaferrites have been studied by employing microwave-assisted sol-gel method.

2 Experimental

The analytically pure of $Sr(NO_3)_2 \bullet 3H_2O$, $La(NO_3)_3 \bullet 6H_2O$, $Fe(NO_3)_3 \bullet 9H_2O$ and citric acid with stoichiometric amounts were dissolved in a certain amount of deionized water. After the solution was stirred homogeneously at 80 °C, the pH value was adjusted to 6 through aqua ammonia solution. The heating and stirring process continued until it formed a viscous dark-green sol. Subsequently, the sol was dried at 120 °C to be brown gel. The self-combustion process took place at 175 °C and the gray fluffy precursor formed. The precursor was calcined at 800 °C

✉ Zhanyong Wang
zhanyong.wang@vip.sina.com

[1] School of Materials Science and Engineering, Shanghai Institute of Technology, Shanghai 201418, China

[2] State Key Laboratory for Advanced Metals and Materials, University of Science and Technology Beijing, Beijing 100083, China

for 80 min in microwave furnace with a heating rate of 40 °C/min. The Setaram labsys TG/DSC was applied to detect the phase transformation of precursor with a heating rate 20 °C/min. The crystal structure of calcined samples was detected by D/max-2000 X-ray diffraction with Cu Ka radiation. The phase volume percent was calculated on the basis of the highest diffraction peaks intensity of the different phases from the XRD patterns. The magnetic properties were measured via the vibrating sample magnetometer (VSM) with a maximum applied magnetic field of 1.8 T at room temperature.

3 Results and Discussion

Figure 1 illustrates the TG/DSC curves of the $Sr_{1-x}La_xFe_{12}O_{19}$ ($x = 0.15, 0.25, 0.5$) precursors. The weight loss appears at 100 °C deriving from the evaporation of free water and bound water in the precursors. A precipitous exothermic peak is observed from 250 to 425 °C, which can be attributed to the citrates decomposition and the formation of metal oxides. Weight loss also occurs from 580 to 800 °C, accompanied with a minor exothermic peak at about 780 °C, which suggests the formation of M-strontium ferrite [16, 17]. Those curves show that the substitution of La^{3+} almost has no effect on the phase transition temperature of the precursors. According to our previous study [16, 18], the precursors are calcined at 800 °C for 80 min in microwave furnace.

Figure 2 shows the XRD patterns of $Sr_{1-x}La_xFe_{12}O_{19}$ ($x = 0, 0.15, 0.25, 0.5$) powders with microwave-assisted calcination at 800 °C for 80 min. A strong diffraction peak of $SrFe_{12}O_{19}$ phase is detected in all the samples. The single $SrFe_{12}O_{19}$ hexaferrite has been identified with the La^{3+}

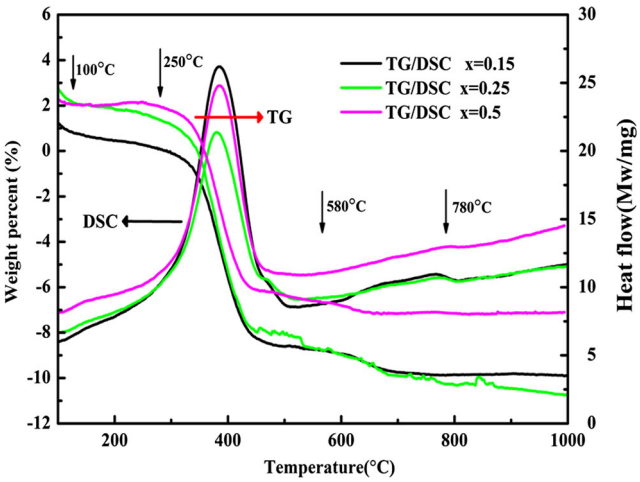

Fig. 1 TG/DSC curves of $Sr_{1-x}La_xFe_{12}O_{19}$ ($x = 0.15, 0.25, 0.5$) precursors

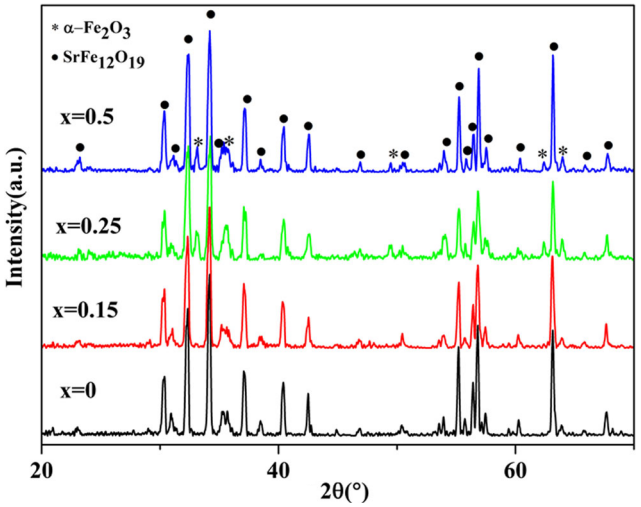

Fig. 2 X-ray diffraction patterns of the $Sr_{1-x}La_xFe_{12}O_{19}$ ($x = 0$, 0.15, 0.25, 0.5) powders

substitution at $x = 0.15$. The diffraction peaks of α-Fe_2O_3 phases are observed in the samples with $x = 0.25$ and 0.5, respectively. Comparing the ionic radius of Sr^{2+} (1.27 Å) with La^{3+} (1.22 Å), the Sr^{2+} substitution by smaller ionic radius La^{3+} could reduce the cell volume. Table 1 lists the lattice constants of $Sr_{1-x}La_xFe_{12}O_{19}$ ($x = 0$, 0.15, 0.25, 0.5) and the volume percentage of α-Fe_2O_3. The lattice constant a and c are calculated by Formula (1), where d_{hkl} represents the crystal distance and (h k l) is the Miller indices.

$$d_{(hkl)} = \left(\frac{4}{3}\frac{h^2 + hk + k^2}{a^2} + \frac{l^2}{c^2}\right)^{-\frac{1}{2}} \quad (1)$$

It indicates that the lattice constant c of strontium ferrites unsubstituted with La^{3+} is bigger than that of substituted samples, because the smaller ionic radius of La^{3+} would reduce the distance along c-axis of the stacking fault, while the lattice constant a has a different change. The mössbauer spectra analysis has figured out that the substitution of Sr^{2+} by La^{3+} is accompanied with the change of Fe^{3+}(0.64 Å) to Fe^{2+}(0.75 Å) at 2a or $4f_2$ crystallographic sites to keep the electrical neutrality of strontium hexaferrite [19]. The Fe^{2+} ions have a large ionic radius than Fe^{3+} ions, which results in the enlargement of the lattice constant a. The volume percentage of α-Fe_2O_3 decrease to 10.5 % after reaching to

Table 1 Lattice constants of $Sr_{1-x}La_xFe_{12}O_{19}$ ($x = 0$, 0.15, 0.25, 0.5) and the volume percentage of α-Fe_2O_3

x	0	0.15	0.25	0.5
a (Å)	5.883	5.882	5.872	5.879
c (Å)	23.065	23.055	23.012	22.964
$\alpha-Fe_2O_3$	–	–	21.1 %	10.5 %

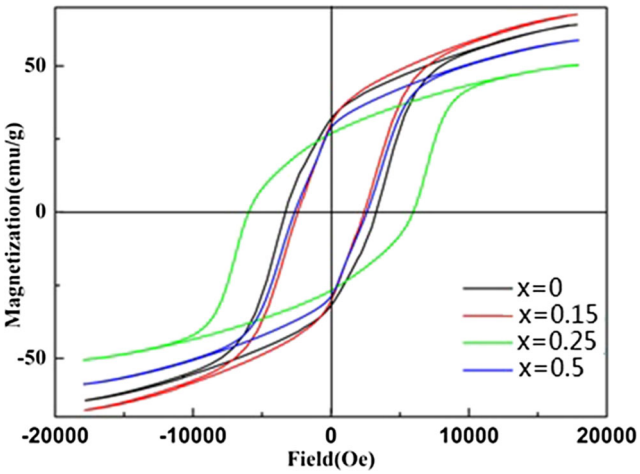

Fig. 3 The hysteresis loops of $Sr_{1-x}La_xFe_{12}O_{19}$ ($x = 0$, 0.15, 0.25, 0.5) powders at room temperature

21.1 % at $x = 0.25$, which is different from the substitution by Pr^{3+} and Dy^{3+} [16].

Figure 3 shows the hysteresis loops of $Sr_{1-x}La_xFe_{12}O_{19}$ ($x = 0$, 0.15, 0.25, 0.5) powders at room temperature. The saturation magnetization (σ_s) increases slightly with the La^{3+} doping content improvement, accompanied with the slight decrease in coercivity. As reported, some reasons have been discussed for the effects of the La^3 substitution. When a divalent Sr^{2+} is replaced by a trivalent La^{3+}, Fe^3 would be converted to Fe^{2+} to maintain the electrical neutrality. The emergence of Fe^{2+} could cause the decrease of net magnetic moment in $Sr_{1-x}La_xFe_{12}O_{19}$ for the valence change of Fe^{3+} to Fe^{2+}, the spin canting deviating from the collinear to non-collinear arrangement, and the weaker super-exchange of Fe^{3+}–O^{2-}–Fe^{2+} [6, 20]. Those combined effects could cause the degradation in σ_s. The substitution of Sr^{2+} by La^{3+} with smaller ionic radius leads to the reduction of lattice constant c [20, 21], as shown in Table 1, which causes the decrease of the Fe–O distance that is parallel to the c-axis. The superexchange interaction of Fe^{3+}–O^{2-}–Fe^{3+} increases at the 12k and 2b site, corresponding with the improvement of σ_s. For the sample with La^{3+} substitution at $x = 0.15$, the stronger superexchange interaction of Fe^{3+}–O^{2-}–Fe^3 could be dominant factor for the slight increase of σ_s. As listed in Table 2, the ratio of σ_r/σ_s is 0.447 with La^{3+} substitution at $x = 0.15$, showing its magnetic multi-domain structure [22]. The magnetization of samples with multi-domain structure is mainly determined by the domain wall displacement. The movement of multi-domain walls is much easier than flipping the magnetization of an entire particle coherently which is the magnetization mechanism of single domain, so the multi-domain grain has lower coercivity. For the sample at $x = 0.25$, the σ_s reduces to 50.449 emu/g. The decrease of σ_s and σ_r could be attributed to the presence of the α-Fe_2O_3 phase. The content of α-Fe_2O_3 is about 21.1 % and it dilutes the magnetization values. The ratio of σ_r/σ_s is 0.532 and a remanence enhancement effect is observed. The exchange coupling effects take place between the hard magnetic $SrFe_{12}O_{19}$ phase and soft magnetic α-Fe_2O_3 phase and the smooth hysteresis loop also verify the effect. This coupling could hide the domain rotation and block the displacement of domain walls. The grain size calculated by scherrer formula at $x = 0.25$ for La^{3+} substitution has only 29.5 nm, resulting in higher coercivity. The ratio of σ_r/σ_s is 0.493 at $x = 0.5$ and the grain has no interaction when the value ratio of σ_r/σ_s below the 0.5. The σ_s and σ_r increased at $x = 0.5$ because of the lower phase composition of α-Fe_2O_3 (Table 1).

Table 2 The grain size and magnetic properties of $Sr_{1-x}La_xFe_{12}O_{19}$ ($x = 0$, 0.15, 0.25, 0.5)

x	0	0.15	0.25	0.5
Grain size (nm)	38.3	31.7	29.5	34.2
σ_r/σ_s	0.497	0.447	0.532	0.493

4 Conclusion

$Sr_{1-x}La_xFe_{12}O_{19}$ ($x = 0$, 0.15, 0.25, 0.5) hexaferrites were prepared by microwave-assisted sol-gel method. The grain size of strontium ferrite reduces when the La^{3+} doping content below $x = 0.25$. The substitution of La^{3+} can remarkably improve the coercivity to 5960.2 Oe at $x = 0.25$. This derived from the fine grain and exchange coupling between the higher volume percentage of α-Fe_2O_3 and the strontium ferrite with signal domain.

Acknowledgments This work was supported by Project of the Shanghai Education Commission of PR China (14ZZ165) and State Key Laboratory for Advanced Metals and Materials of PR China (2013-Z02).

References

1. Nga, T.T.V., Duong, N.P., Hien, T.D.: J. Magn. Magn. Mater. **324**, 1141 (2012)
2. Sharma, P., Verma, A., Sighu, R.K., Pandey, O.P.: J. Alloys Compd. **361**, 257 (2003)
3. Li, Y.Q., Huang, Y., Qi, S.H., Niu, L., Zhang, Y.L., Wu, Y.F.: Appl. Surf. Sci. **258**, 3659 (2012)
4. Jiang, J., Ai, L.H.: J. Alloys Compd. **502**, 488 (2010)
5. Wang, W.T., Li, Q.L., Chang, C.B.: Synth. Met. **161**, 44 (2011)
6. Iqbal, M.J., Farooq, S.: Mater. Res. Bull. **46**, 662 (2011)
7. Rai, B.K., Mishra, S.R., Nguyen, V.V., Liu, J.P.: J. Alloys Compd. **550**, 198 (2013)
8. Feng, J., Matsushita, N., Wantanabe, K., Nakagawa, S., Naoe, M.: J. Appl. Phys. **85**, 6139 (1999)

9. Kazin, P.E., Trusov, L.A., Zaitsev, D.D., Tretyakov, Y.D., Jansen, M.: J. Magn. Magn. Mater. **320**, 1068 (2008)
10. Wang, S., Ding, J., Shi, Y., Chen, Y.J.: J. Magn. Magn. Mater. **219**, 206 (2000)
11. Baghbanzadeh, M., Carbone, L., Cozzoli, P.D., Kappe, C.O.: Angew. Chem. Int. Edit. **50**, 11312 (2011)
12. Gedye, R., Smith, F., Westaway, K., Ali, H., Baldisera, L., Laberge, L., Rousell, J.: Tetrahedron Lett. **27**, 279 (1986)
13. Giguere, R.J., Bray, T.L., Duncan, S.M., Majetich, G.: Tetrahedron Lett. **27**, 4945 (1986)
14. Zhu, Y.J., Wang, W.W., Qi, R.J., Hu, X.L.: Angew. Chem. Int. Edit. **43**, 1410 (2004)
15. Yu, J., Shen, C.Y.: Electronic Components and Materials **34**, 1 (2015). (in Chinese)
16. Zhou, Z.P., Wang, Z.Y., Wang, X.T., Wang, X.R., Zhang, J.S., Dou, F.K., Jin, M.L., Xu, J.Y.: J. Alloys Compd. **610**, 264 (2014)
17. Surig, C., Hempel, K.A., Bonnenberg, D.: IEEE Trans. Magn. **30**, 4092 (1994)
18. Wang, Z.Y., Zhong, L.M., Lv, J.L., Qian, H.C., Zheng, Y.L., Fang, Y.Z., Jin, M.L., Xu, J.Y.: J. Magn. Magn. Mater. **322**, 2782 (2010)
19. Seifert, D., Töpfer, J., Stadelbauer, M., Grössinger, R., Breton, J., Le, M.: J. Am. Ceram. Soc. **942**, 109 (2011)
20. Liu, X., Zhong, W., Yang, S., Yu, Z., Gu, B., Du, Y.: J. Magn. Magn, Mater. **238**, 207 (2002)
21. Qiao, L., You, L.S., Zheng, J.W., Jiang, L.Q., Sheng, J.W.: J. Magn. Magn. Mater. **318**, 74 (2007)
22. Zi, Z.F., Sun, Y.P., Zhu, X.B., Yang, Z.R., Dai, J.M., Song, W.H.: J. Magn. Magn. Mater. **320**, 2746 (2008)